The significance of the Quantum Volume for other algorithms: a case study for Quantum Amplitude Estimation*

Jins de Jong[1] and Carmen R. Hoek[1]

TNO, Unit ISP, Zernikelaan 14, 9747AA Groningen, The Netherlands
jins.dejong@tno.nl

Abstract. The quantum volume is a comprehensive, single number metric to describe the computational power of a quantum computer. It has grown exponentially in the recent past. In this study we will assume this remains the case and translate this development into the performance development of another quantum algorithms, quantum amplitude estimation. This is done using a noise model that estimates the error probability of a single run of an algorithm. Its parameters are related to the quantum volume under the model's assumptions.
Applying the same noise model to quantum amplitude estimation, it is possible to relate the error rate to the generated Fisher information per second, which is the main performance metric of quantum amplitude estimation as a numerical integration technique. This provides a prediction of its integration capabilities and shows that quantum amplitude estimation as a numerical integration technique will not provide an advantage over classical alternatives in the near future without major breakthroughs.

Keywords: Quantum volume · Quantum amplitude estimation · Noisy quantum computing.

1 Introduction

The promise of the quantum computer is that it can speed up some computation routines quadratically or can even solve classically intractable problems with an exponential speed-up. The capabilities of current quantum computers are limited by errors rather than by size or speed. The origin of these errors lies in the details of their physical realization. Given that there are multiple physical approaches to build a quantum computer, each with different components, strengths and weaknesses, it is hard to compare quantum computers' performance on an algorithm from the reported error characteristics of the physical components. To obtain more understanding of the execution quality, performance metrics focus increasingly on application benchmarks [16,18,19]. These use the size, speed or

* This work was supported by the Dutch National Growth Fund (NGF), as part of the Quantum Delta NL programme.

ICCS Camera Ready Version 2024
To cite this paper please use the final published version:
DOI: 10.1007/978-3-031-63778-0_16

solution quality of an application on a quantum machine as metric. Currently, the most reported metric of this kind is the quantum volume (QV) [7].

This paper studies the implications of the development of the QV for the quantum amplitude estimation (QAE) algorithm. Can the available QV be translated into a performance estimate for QAE?

1.1 Quantum volume

Using application-based metrics rather than component properties to benchmark the performance of a quantum processing units (QPU) provides a view on the performance that is of direct interest for the user. The best-known metric of this kind today is the quantum volume. It gives in a single number the size of a specific computational problem, finding the heavy outputs of a randomized circuit, that can be run reliably.

The QV metric considers both the width of the machine and the depth of the circuit that is run. Circuits that are too wide, do not fit onto the available number of qubits. If the circuit becomes too deep, a run of the circuit becomes unreliable as a result of errors in the gate execution. The QV is the largest size of the problem that can be run on a quantum machine, without being dominated by noise. As such, it is a property of the hardware. In most current designs of quantum computers, the depth is the bottleneck for the development of the QV.

The QV will not remain the common performance metric in the future. Noiseless executions of the circuits are needed to determine the QV. In the near future these can only be performed using long-lasting simulations on classical hardware. These simulations will take so lang that for such QPU's alternative metrics, such as the Error per layered gate [30], will be needed.

1.2 QAE as a numerical integration technique

On a quantum computer, numerical integration can be performed with quantum amplitude estimation (QAE) algorithms [25,15,27,11]. Compared to the classical algorithms, QAE enjoys faster convergence rates in ideal, noiseless settings. Furthermore, it may function on near-term NISQ devices [22,26]. This paper aims to study if these convergence rates are feasible on near-term quantum hardware.

For this we compare QAE with the Monte Carlo integration (MCI) technique for classical computers. In MCI a random sample from the domain is chosen and its average function value is multiplied by the volume of the domain as an estimate of the integral. Since the function is evaluated once for each sample point, the number of function evaluations N is the same as the number of samples. The error of MCI decreases as $N^{-1/2}$ [24]. The accuracy of this method is determined only by the number of samples that is processed.

ICCS Camera Ready Version 2024
To cite this paper please use the final published version:
DOI: 10.1007/978-3-031-63778-0_16

Both MCI and QAE treat a finite number of samples. Thus, the sampling error is present too in QAE. In the approach [25] used here, a circuit of $n+1$ qubits generates 2^n samples. QAE can only be beneficial, if $2^n > N$, where N is the number of MCI samples. The classical example in section 2.6 suggests 2^{26} samples are needed for this, so quantum computers with at least 27 qubits are needed [25]. This puts a lower bound on the QV required to perform competitive QAE.

Besides this sampling error, the quantum computer suffers from other errors inherent to the quantum process. The challenge is thus to device a method for which the quantum errors decay faster than $N^{-1/2}$, where N is interpreted as the number of function evaluations.

1.3 Related work

The quantum volume [7,4] is shown to be a suitable candidate for a quantum metric by [3]. Limitations of randomized application-centric benchmarks have been studied in [23]. An exponential growth of the quantum volume has been observed, since its conception [9].

The QAE algorithm is based on the quantum phase estimation algorithm [5,8]. Replacing the quantum Fourier transform with maximum likelihood estimation [25] simplifies the circuit considerably. A method without post-processing is Iterative QAE [12] at the price of a varying execution length. Generalizations for real-valued integrands [17] or minimal circuit depth [13] have also been constructed. To avoid very deep circuits, maximum-depth approximations have been tested in the noiseless setting [21]. The performance of QAE in the presence of noise has been studied in [6,28,26].

1.4 Our contributions

How can a user estimate the performance of a quantum algorithm from the available QV? We try to provide a first answer to this question. To this end a noise metric will be used that can be derived from the QV. It gives for a single circuit run an estimate of the error rate as a function of the size of the transpiled and decomposed circuit and the number of measurements.

A second contribution lies in the application of this method to QAE. The QAE algorithm of [25] looks very promising [20], but it is unclear when it will outperform classical integration methods. The observed exponential growth of the quantum volume can be translated into error parameters for QAE runs. Using these, predictions for the Fisher information per second can be made, which is the metric that determines the accuracy. These shows that major breakthroughs are needed to make QAE competitive with classical methods in the near future.

ICCS Camera Ready Version 2024
To cite this paper please use the final published version:
DOI: 10.1007/978-3-031-63778-0_16

This article is structured as follows. In section 2 an introduction of the QV, our noise model and QAE is given. The theoretical relation between the noise model and the quantum volume, as well as an applicability test of our noise model are given in section 3. These are combined with the size characteristics of the QAE and QV circuits in section 4 to provide an estimate of the integration power of QAE in the near future. The paper is concluded with section 5.

2 Preliminaries

This section briefly treats the concept of QV, introduces our noise model with its assumptions and summarizes the framework of QAE and Fisher information for noiseless and noisy quantum processors.

The quantum volume of a QPU with N available qubits is determined from a set of experiments on squared circuits, meaning that the number of qubits q used is equal to the number of randomized layers, where $q = 1, 2, \ldots, N$. In each layer, the qubits are permuted randomly, divided into pairs that are rotated with a random element of $SU(4)$. Such a circuit on q qubits will return on measurement each q-bit answer with a certain probability. By definition, half of the answers will have a probability larger than the median. These are called the heavy outputs. The idea of a QV experiment is to reproduce as many of these heavy outputs using the noisy quantum computer. An ideal machine would produce 84.66% of the heavy outputs [3] and guessing would yield half of the heavy outputs. A quantum volume experiment is defined [7] to be successful if 2/3 of the heavy outputs is found with a one-sided 2σ certainty. The quantum volume is the largest layer depth q for which the experiments is successful.

To estimate when certain algorithms become feasible on a quantum computer one could look to the evolution of quantum volume. IBM reached a quantum volume of 512 with its Prague machine [10], which corresponds approximately to a doubling of the quantum volume every 9 months since 2018 [14]. Based on [1] one would deduce that the quantum volume doubles every 4 months for Quantinuum systems since June 2020. There are estimates [9] that the quantum volume has doubled approximately every 6 months since its conception, which is what we will use as a forecast

$$V_Q(T) = 2^{2+T/6} \,, \tag{1}$$

where T is the time in months since November 2018. In section 1.2 it was estimated that 27 qubits may suffice. Based on (1) a reliable machine to execute QV circuits with 27 qubits may be available in May 2031. According to IBM's roadmap [2], circuits of 10^9 gates should be feasible then. However, the error sensitivity and implementation size of QAE circuits is different.

ICCS Camera Ready Version 2024
To cite this paper please use the final published version:
DOI: 10.1007/978-3-031-63778-0_16

2.1 The noise model

Quantum processors are not deterministic, so statements regarding the quality of an algorithm run must be statistical. In addition, current QPU's are noisy, meaning that the execution of gates succeeds with a probability strictly smaller than 1. It follows that results on the probability of an error occurrence must be derived from statistics of the observations, the expected noiseless outcomes and the expected outcomes with noise. However, describing the outcome in the case of a faulty gate execution is very cumbersome, if possible at all. To avoid this, we make the simplifying assumption that a uniformly random answer is measured upon an error. In other words, if an error occurs, we assume that all structure is lost and a random output will be measured.

Half of the outcomes of a QV circuit are heavy outputs and in the QAE circuits of [25] only one qubit is measured. So, in both algorithms errors reduce the assumed success probability of a measurement to 0.5. Under this assumption, if i should be measured with probability p_i in a noiseless case and the probability of an error occurring is $1-a$, upon measurements i will be found with probability

$$p_i' = ap_i + 0.5 \cdot (1-a) \; .$$

Most sources of errors lead to similar behavior of QV experiments [4]. As a simplification, only two sources of error will be considered, the execution of the gates and the measurements. The probability of a successful measurement of a qubit will be given by b and the probability that 100 gates are executed correctly by c. Based on two parameters, the number m of measurements and the size s of the circuit, decomposed in the basis gates and transpiled into the topology of the hardware, this yields a total probability of an error-free run of

$$a = b^m \cdot c^{s/100} \; . \tag{2}$$

In practice, b will be close to 1.0 and the number of measured qubits q small, so that the formula is dominated by the second factor. In a different context, such assumptions have been applied to QAE in [28,6,26].

2.2 QAE without noise

To apply the noise model to the QAE algorithm, we recall some results on the Fisher information for the noiseless and noisy case. The implementation used in this study is based on [25], because its implementation is shallow and has a size that is known upfront.

ICCS Camera Ready Version 2024
To cite this paper please use the final published version:
DOI: 10.1007/978-3-031-63778-0_16

The numerical integral we study is given by

$$\begin{aligned} I[f] &= \int_0^1 \mathrm{d}x\, f(x)p(x) \\ &\approx \mathbb{E}_p[f] = \frac{1}{2^q}\sum_{x=0}^{2^q-1} f(\frac{x}{2^q})\, p(\frac{x}{2^q}) \qquad (3) \\ &=: \sin^2\vartheta\ . \qquad (4) \end{aligned}$$

It is assumed that the function f can be shifted and scaled, so that $0 \leq I[f] \leq 1$ and an angle $\vartheta \in [0, \pi/2]$ exists satisfying (4). It is this angle that the QAE algorithm computes.

The probability distribution on the q qubits is implemented by the unitary

$$\mathcal{P} : |0\rangle_q \mapsto \sum_{x=0}^{2^q-1} \sqrt{p(x)}|x\rangle_q$$

and the function f is implemented by a unitary operator $\mathcal{R}$ on $q+1$ qubits

$$\mathcal{R} : |x\rangle_q|0\rangle \mapsto |x\rangle_q\big(\sqrt{f(x)}|1\rangle + \sqrt{1-f(x)}|0\rangle\big)\ .$$

Together, these operators define $\mathcal{A} = \mathcal{R}(\mathcal{P}\otimes 1)$. This is the state preparation

$$|\Psi\rangle = \mathcal{A}|0\rangle_{q+1} = \sin\vartheta|\Psi_1\rangle|1\rangle + \cos\vartheta|\Psi_0\rangle|0\rangle\ ,$$

which is split into a good state Ψ_1 and a bad state Ψ_0. Upon measurement of the last qubit, the probability to find $|1\rangle$ is

$$\sin^2\vartheta = \sum_{x=0}^{2^q-1} p(x)f(x)\ .$$

In order to generate a quantum speed-up, an amplification operator is needed. This operator is defined [25] as $Q = -\mathcal{A}S_0\mathcal{A}^{-1}S_{\Psi_1}$. The operators

$$S_0 : |0\rangle_{q+1} \mapsto -|0\rangle_{q+1} \quad \text{and} \quad S_{\Psi_1} : |\Psi_1\rangle|1\rangle \mapsto -|\Psi_1\rangle|1\rangle$$

and act trivially on other states. It follows that the operator $\mathcal{A}$ is a rotation, so that

$$Q^k|\Psi\rangle = \sin((2k+1)\vartheta)|\Psi_1\rangle|1\rangle + \cos((2k+1)\vartheta)|\Psi_0\rangle|0\rangle\ .$$

The amplification operator Q contains both $\mathcal{A}$ and $\mathcal{A}^{-1}$, so that operating Q once counts as two function evaluations. After k amplification steps there are $2k+1$ function evaluations performed. Because the amplified angles provide more information about the value of ϑ [25,6], amplification increases the efficiency and constitutes the potential quantum advantage of QAE.

ICCS Camera Ready Version 2024
To cite this paper please use the final published version:
DOI: 10.1007/978-3-031-63778-0_16

After the circuits have been run for a selection of amplification powers, the angle ϑ must be derived from the outcomes. For each amplification power $k \in \mathcal{M}$, N_k shots are performed with h_k measurements of 1. The best choice for ϑ is the one that maximizes the likelihood

$$L(\vartheta) = \prod_{k \in \mathcal{M}} \Big(\sin^2((2k+1)\vartheta)\Big)^{h_k} \times \Big(\cos^2((2k+1)\vartheta)\Big)^{N_k - h_k} .$$

2.3 QAE on noisy processors

On a noiseless QPU more amplification rounds result in more information. For noisy processors the situation is more complex [28]. Larger amplification powers yield larger circuits and more noise, reducing the amount of extractable information. The challenge is to optimize the amount of generated information based on the error parameters of the QPU.

Before the noise model (2) can be used, it should be validated whether it can be used to explain the observed noisy measurements. This is done by using small dummy QAE circuits, because complete QAE circuits are too large and the outcomes would be dominated by noise. These dummy QAE circuits can be simulated without errors to obtain the noiseless outcomes p_i of measuring a state i. Repeating the experiments on a noisy QPU provides the noisy outcomes p'_i. Afterwards, the best fitting probability a is found that minimizes

$$V_1 = \sum_{i=1}^{2} \big(p'_i - (ap_i + \frac{1-a}{2})\big)^2 = -\frac{(a-1)^2}{2} + \sum_i (p'_i - ap_i)^2 ,$$

which is solved by

$$a = \frac{2p'_1 - 1}{2p_1 - 1} . \tag{5}$$

This means that the error probability, the noisy and the noiseless probabilities are related by

$$p'_i = ap_i + \frac{1-a}{n} .$$

The ratio of V_1 against $V_0 = \sum_{i=1}^{2}(p'_i - p_i)^2$ can be used to describe the quality of the noise model. It is given by $\mathcal{R}^2 = 1 - \frac{V_1}{V_0}$.

The interpretation as a probability dictates that $a \in [0, 1]$, but fluctuations in the measurement results may lead to solutions of (5) outside this interval. Both $p'_0 > p_0 > 0.5$ and $p'_0 < p_0 < 0.5$ imply $a > 1$. Negative values of a are observed for $p'_0 < 0.5 < p_0$ and $p_0 < 0.5 < p'_0$. Noise should drive the observed noisy probabilities p'_i from p_i towards 0.5, but statistical fluctuations may lead to negative values for single experiments.

ICCS Camera Ready Version 2024
To cite this paper please use the final published version:
DOI: 10.1007/978-3-031-63778-0_16

2.4 Dummy QAE circuits

Standard QAE circuits are too deep to run on available noisy hardware and are thus unsuited to validate the noise model. Therefore, dummy QAE circuits composed of the same gates are used. Such circuits consist of R rounds of not-gates and one multi-controlled y-rotation. The rotation acts on the last qubit and is controlled by randomly selected qubits, flipped to 1 and back after the rotation. Only the last qubit is measured. The tests are run on IBM-perth (7 qubits) and the results are used to fit the noise model. The results are shown in section 3.2. Tests have also been run on IBM-guadalupe (16 qubits), but these circuits are so large that all obtained values of a will be effectively zero and prevent fitting.

Besides IBM-perth and IBM-guadalupe, it is useful to run the circuits on quantum processors of intermediate sizes. Therefore, simulations with a noise model have been performed on a series of topologies for 8 until 12 qubits that interpolate between IBM-perth and IBM-guadalupe. The idea behind the choices is that the topology should have a similar influence on the observed noise parameters in all the experiments. Since these are not available as hardware, the noise effects are simulated with a thermal noise model that mimics the noise characteristics of IBM-perth.

2.5 Fisher information

The amount of information generated by a numerical integration method is given by the Fisher information $\mathcal{I}$. Its relevance follows from the Cramer-Rao bound

$$\mathrm{Var}(\vartheta) \geq \frac{1}{\mathcal{I}(\vartheta)}$$

which is an equality for this approach of QAE [25]. For QAE with depolarizing noise it can be derived [6,28] from the noiseless case. Writing the noiseless and noisy probabilities for k amplification rounds as $p_{(k)} = \cos^2(2k+1)\vartheta$ and $p'_{(k)} = a_k p_{(k)} + \frac{1-a_k}{2}$, the Fisher information is given by

$$\mathcal{I}(\vartheta) = \sum_{k\in\mathcal{M}} \frac{a_k^2 N_k (2k+1)^2}{p_{(0)}(1-p_{(0)})} \frac{p_{(k)}(1-p_{(k)})}{p'_{(k)}(1-p'_{(k)})} \,. \tag{6}$$

The angle ϑ is obtained through maximization of the noisy likelihood function

$$\mathcal{L}'(\vartheta) = \prod_{k\in\mathcal{M}} (p'_{(k)})^{h_k} (1-p'_{(k)})^{N_k - h_k} \,.$$

The formulas above show that the value $\vartheta = \pi/4$ is of particular interest. In this case $p_{(k)} = p'_{(k)} = 1/2$, so that the error parameters are irrelevant and the Fisher information is maximal. QAE problems are ideally formulated in a way that the expected angle is close to $\pi/4$, so that

$$\mathcal{I}(\vartheta) = 4b \sum_k (2k+1) c^{2k} \cdot \big(N_k(2k+1)\big) \,. \tag{7}$$

ICCS Camera Ready Version 2024
To cite this paper please use the final published version:
DOI: 10.1007/978-3-031-63778-0_16

Maximizing this against the available number of function evaluations $M = \sum_k N_k(2k+1)$ yields $N_{k_1} = \frac{M}{2k_1+1}$, where k_1 maximizes $(2k+1)c^{2k}$. To determine precisely when to switch from $k-1 \to k$ amplification steps, solve

$$(2k+1)c^{2k} \geq (2k-1)c^{2k-2} \qquad \Rightarrow \qquad k = \left\lfloor \frac{1}{1-c^2} - \frac{1}{2} \right\rfloor . \tag{8}$$

2.6 A Monte Carlo example

The interest in QAE comes from its ability to converge faster than MCI, so a simple estimate of the reference speed of MCI is useful to choose the parameters of the quantum algorithm. For this purpose a 1D integral is determined numerically with $N = 10^7$ samples in 47.4 seconds on a legacy processor, estimated at 0.2 Tflops. In an operational setting, a computing cluster of 100 Tflops could thus evaluate approximately 10^8 samples per second. MCI works without amplification, so the Fisher information per second is $4 \cdot 10^8$, according to (7).

3 Results

3.1 Success in a quantum volume experiment

The probability to find a heavy output on an ideal QPU is $r = 0.8466$ [3]. In a QV experiment on a noisy QPU with q qubits a heavy output will be found with probability $r' \leq r$ with variance $r'(1-r')$. After N measurements, the experiment has passed the test, if

$$\frac{2N}{3} + 2\sigma \leq Nr' \quad \Rightarrow \quad r'(1-r') \leq \frac{N}{4}(r' - \frac{2}{3})^2 ,$$

so a QV experiment can succeed as long as $r' > \frac{2}{3}$. Since half of the states are heavy outputs and we assume to measure a random state if an error occurs,

$$r' = ar + \frac{1-a}{2} .$$

A QV experiment will fail, if the probability of an error-free run drops below

$$a_Q = \frac{r' - 1/2}{r - 1/2} = 0.4809 . \tag{9}$$

From the values r' and r the value of the error parameter a can be derived, which we attempt to model by (2) with $m = q$.

3.2 Results for the error model

To test the assumptions behind the noise model dummy QAE circuits are run on real and simulated hardware. The results are used to fit the parameters of the noise model (2) with $m = 1$. The quality of the resulting model can then

ICCS Camera Ready Version 2024
To cite this paper please use the final published version:
DOI: 10.1007/978-3-031-63778-0_16

be expressed by the $\mathcal{R}^2$-score. The obtained results are presented in Table 1. To test whether this noise model also works for more qubits, the procedure has been repeated for larger simulated machines with a modified thermal noise model. This causes the difference between the values for c in Figure 1 and the value found in (the caption of) Table 1.

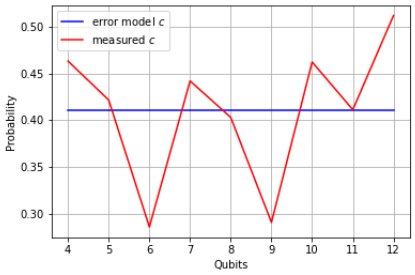

Fig. 1: The error per 100 gates c versus the number of qubits in the circuit. The average value of $b = 0.9958$. The dummy QAE circuits used here are discussed in paragraph 2.4. All experiments are simulated using a modified thermal noise model.

Rounds	Tests	Depth	Size	a	$\tilde{a}$
0	20	1.0	1.0	0.938	0.923
1	20	74.2	99.3	0.278	0.351
2	20	144.5	202.8	0.233	0.127
3	20	206.7	294.8	0.010	0.051
4	20	290.6	408.4	0.044	0.017
5	20	348.5	495.8	0.093	0.007
6	20	401.4	570.5	-0.044	0.003
7	20	497.5	725.5	0.056	0.001

Table 1: The results for dummy QAE circuits on IBM-perth (7 qubits). The obtained parameters for (2) are $b = 0.938$ and $c = 0.374$. The average probability for an error-free run is given by a, its prediction by (2) is $\tilde{a}$. This noise model can explain $\mathcal{R}^2 = 0.75$ of the variance in the data.

3.3 Speed of the QPU

The unit of speed of IBM's quantum computers is the circuit layer operations per second [29] or CLOPS. This gives the number of layers of a QV circuit it can process per second. The size in gates of the transpiled and decomposed QV circuits can be determined to translate this speed metric into one applicable to other quantum circuits. This shows the $2.9K$ clops of IBM-perth corresponds to

$$\mathcal{S} = 1.0 \times 10^6 \pm 0.6 \times 10^6 \text{ basis gate operations per second.} \tag{10}$$

3.4 Estimations for the size of circuits

Within the frame of the noise model of paragraph 2.1, the size of the circuit is the dominant parameter. We need, therefore, the scaling of the size of the circuits for more qubits. The size S_1 of a QAE circuit as a function of the number of qubits q and the number of amplification rounds R is

$$S_1 = \alpha_1 \cdot (2R + 1) \cdot 10^{\beta_1 \cdot q} \quad \text{with } \alpha_1 = 17.35 \text{ and } \beta_1 = 0.46\,. \tag{11}$$

ICCS Camera Ready Version 2024
To cite this paper please use the final published version:
DOI: 10.1007/978-3-031-63778-0_16

The size of the QV circuit depends on the number of qubits only, since it is squared. The depth in layers is equal to the number of qubits. Because the circuit need to be transpiled, a quadratic relation between the number of qubits and the depth of the circuit is obtained, which implies a cubic relation between the number of qubits and the size of the circuit. This relation is given by

$$S_2 = \alpha_2 \cdot q^3 + \beta_2 \cdot q^2 \quad \text{with } \alpha_2 = 0.24 \text{ and } \beta_2 = 8.13. \tag{12}$$

4 Application of the noise model to QAE

Now that all elements required are present, they can be combined to sketch the prospect of the integration power of QAE. This is the topic of this section.
The parameters b and c of the noise models for QV and QAE circuits represent properties of the QPU rather than of the circuits run on them. Our claim is that they are the same for both types of circuits. In this way we may translate the development of the QV into an error parameter for a single circuit run. This can then be used to model the Fisher information that a QPU can generate.

4.1 General functions

The number of qubits that can pass a QV experiment (1) is expected to grow as $q(T) = 2 + \frac{T}{6}$. The expected probability $r'(T)$ to run a QV circuit without errors at future time T can be inferred from (1) and (9). In terms of the (gate) size s of a circuit this probability can be modelled as

$$a = b^q c^{\frac{s}{100}} \approx c^{\frac{s}{100}} \ .$$

To simplify the computations it is assumed that $b = 1$. This is justified by the values of b seen in (the captions of) Figure 1 and Table 1.

Expressing the error probability per depth c deduced from a QV experiment with size (12) as a function of $q(T)$ yields

$$c(T) = a_Q^{\frac{100}{\alpha_2 q(T)^3 + \beta_2 q(T)^2}} \ .$$

Combined with the size of a QAE circuit (11) this yields the probability

$$a_{OP}(T) = a_Q^{\frac{\alpha_1 (2R+1) \cdot 10^{\beta_1 Q}}{\alpha_2 q(T)^3 + \beta_2 q(T)^2}} \tag{13}$$

to run a QAE circuit with R amplification rounds on Q qubits without errors.

Each function evaluation takes the same amount of time. The number of amplification rounds that yields the most Fisher information per unit of time is the same as maximizing it per number of function evaluations. The optimal number of amplification rounds (8) then is

$$R(T) = \left\lfloor \left(1 - a_Q^{\frac{2 \cdot \alpha_1 \cdot 10^{\beta_1 Q}}{\alpha_2 q(T) + \beta_2 q(T)^2}}\right)^{-1} - \frac{1}{2} \right\rfloor .$$

ICCS Camera Ready Version 2024
To cite this paper please use the final published version:
DOI: 10.1007/978-3-031-63778-0_16

This leads to an optimal number of amplification rounds shown in Figure 2a and an optimal operational success probability of (13). This probability decreases after the number of amplifications rounds has just increased, but this is compensated by the extra information gained from the experiments. Assuming that

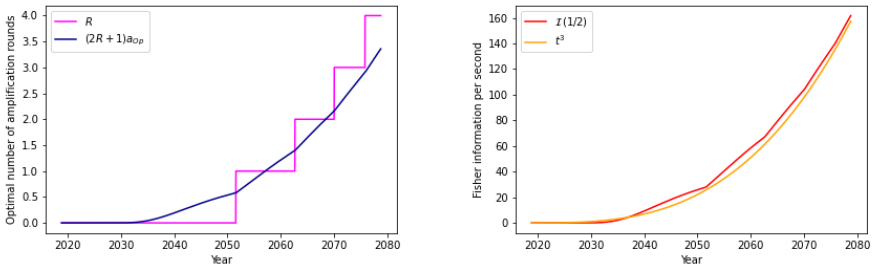

(a) The optimal number of amplification rounds (magenta) and the scaled optimal operational error rate (purple).

(b) The Fisher information per second (red) and the time November 2018 cubed with some prefactor (orange).

Fig. 2: The performance characteristics of QAE on 8 qubits. The length of the x-axis is chosen to show the trends and general development clearly, not to suggest the lifespan of our predictions.

the speed of the QPU's remains constant and is given by (10), the achievable Fisher information per second (7) is given by

$$\mathcal{I}(\frac{1}{2}) = 4 \cdot 1.0 \cdot 10^6 \cdot a_{OP}^2(T) \cdot \frac{\big(2R(T)+1\big)}{\alpha_1 10^{\beta_1 Q}} \ .$$

Figure 2b shows that the Fisher information will increase cubically in time as a function of the exponentially increasing quantum volume. This shows that this approach for QAE will not be competitive in the coming years.

4.2 Shallow functions

Figure 2b shows that the Fisher information increases cubically with time, whereas the QV increases exponentially in time. The implementation of these functions is too deep to yield reliable QAE circuits. Significant improvements are needed to make QAE faster than classical methods. Switching to shallower functions could be an option. And to approximate the 10^8 samples a computing cluster may evaluate, the QAE algorithm should be executed on at least $Q = 27$ qubits. To see the effects of these changes, the analysis of the previous section is repeated here with a hypothetical shallow implementation size of

$$s_3 = 1.0 \cdot (2R+1) \cdot q^3 \ . \tag{14}$$

ICCS Camera Ready Version 2024
To cite this paper please use the final published version:
DOI: 10.1007/978-3-031-63778-0_16

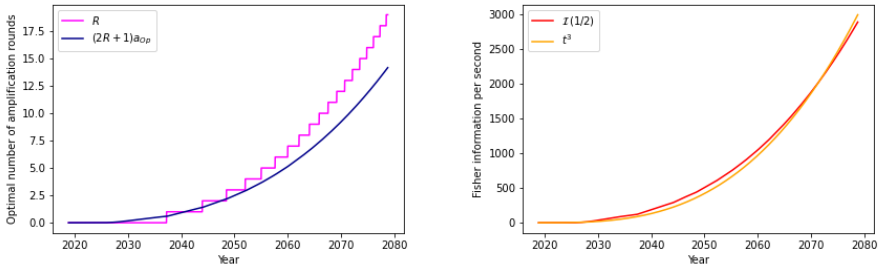

(a) The optimal number of amplification rounds (magenta) and the scaled optimal operational error rate (purple).

(b) The Fisher information per second (red) and the time since November 2018 cubed with some prefactor (orange).

Fig. 3: The performance characteristics of QAE with a shallow function implementation (14) on 27 qubits. The length of the x-axis is chosen to show the trends and general development clearly, not to suggest the lifespan of our predictions.

The results are summarized in Figure 3. This shows that the amount of Fisher information generated per second for shallow circuit implementations of the integrand increases cubically and will remain much lower than for MCI.

5 Conclusions

We have used a phenomenological noise model of measurement and depolarizing noise to model the error probability for a single run of a quantum volume experiment. This same model with the same parameters can be used in the context of other quantum algorithms, such as quantum amplitude estimation. The main parameter of the noise model is the size of the circuit decomposed into basis gates and transpiled for the topology of the quantum processor. Using information on the circuit size, the computational limits of other algorithms can be related directly to the corresponding quantum volume. This provides a novel view on the applicability of such algorithms in the near future.

Applying this method to quantum amplitude estimation, it can be used to estimate to achievable Fisher information per second in the upcoming years. This shows that both for general functions and for (hypothetical) shallow functions the implementation size of the circuit will be prohibitive to achieve an actual quantum advantages. This shows that significant improvements in the QPU are needed to achieve a quantum advantage for quantum amplitude estimation in the NISQ era.

ICCS Camera Ready Version 2024
To cite this paper please use the final published version:
DOI: 10.1007/978-3-031-63778-0_16

Acknowledgements We would like to thank Niels Neumann, Esteban Aguilera, Robert Wezeman and Ward van der Schoot for their contributions to this project.

References

1. Https://metriq.info/
2. (Jan 2024), https://www.ibm.com/roadmaps/quantum.pdf
3. Aaronson, S., Chen, L.: Complexity-Theoretic Foundations of Quantum Supremacy Experiments. In: Proceedings of the 32nd Computational Complexity Conference. CCC '17, Schloss Dagstuhl–Leibniz-Zentrum fuer Informatik, Dagstuhl, DEU (2017). https://doi.org/10.5555/3135595.3135617
4. Baldwin, C.H., Mayer, K., Brown, N.C., Ryan-Anderson, C., Hayes, D.: Re-examining the quantum volume test: Ideal distributions, compiler optimizations, confidence intervals, and scalable resource estimations. Quantum **6**, 707 (May 2022). https://doi.org/10.22331/q-2022-05-09-707, https://doi.org/10.22331/q-2022-05-09-707
5. Brassard, G., Hoyer, P., Mosca, M., Tapp, A.: Quantum Amplitude Amplification and Estimation. AMS Contemporary Mathematics Series **305** (06 2000). https://doi.org/10.1090/conm/305/05215
6. Brown, E.G., Goktas, O., Tham, W.K.: Quantum Amplitude Estimation in the Presence of Noise. arXiv: Quantum Physics (2020). https://doi.org/10.48550/arXiv.2006.14145
7. Cross, A.W., Bishop, L.S., Sheldon, S., Nation, P.D., Gambetta, J.M.: Validating quantum computers using randomized model circuits. Phys. Rev. A **100**, 032328 (Sep 2019). https://doi.org/10.1103/PhysRevA.100.032328
8. D'Ariano, G.M., Macchiavello, C., Sacchi, M.F.: On the general problem of quantum phase estimation. Physics Letters A **248**(2-4), 103–108 (nov 1998). https://doi.org/10.1016/S0375-9601(98)00702-6
9. Ezratty, O.: Understanding Quantum Technologies 2022 (2022). https://doi.org/10.48550/arXiv.2111.15352
10. Gambetta, J.: (2022), https://twitter.com/ jaygambetta/status/1529489786242744320
11. Giurgica-Tiron, T., Kerenidis, I., Labib, F., Prakash, A., Zeng, W.: Low depth algorithms for quantum amplitude estimation. Quantum **6**, 745 (jun 2022). https://doi.org/10.22331/q-2022-06-27-745, https://doi.org/10.22331/q-2022-06-27-745
12. Grinko, D., Gacon, J., Zoufal, C., Woerner, S.: Iterative quantum amplitude estimation. npj Quantum Information **7**, 52 (03 2021). https://doi.org/10.1038/s41534-021-00379-1
13. Herbert, S.: Quantum Monte Carlo Integration: The Full Advantage in Minimal Circuit Depth. Quantum **6**, 823 (Sep 2022). https://doi.org/10.22331/q-2022-09-29-823, https://doi.org/10.22331/q-2022-09-29-823
14. Jurcevic, P., Zajac, D., Stehlik, J., Lauer, I., Mandelbaum, R.: (Apr 2022), https://research.ibm.com/blog/quantum-volume-256
15. de Lejarza, J.J.M., Grossi, M., Cieri, L., Rodrigo, G.: Quantum fourier iterative amplitude estimation. 2023 IEEE International Conference on Quantum Computing and Engineering (QCE) **01**, 571–579 (2023). https://doi.org/10.1109/QCE57702.2023.00071

ICCS Camera Ready Version 2024
To cite this paper please use the final published version:
DOI: 10.1007/978-3-031-63778-0_16

16. Lubinski, T., Johri, S., Varosy, P., Coleman, J., Zhao, L., Necaise, J., Baldwin, C.H., Mayer, K., Proctor, T.: Application-oriented performance benchmarks for quantum computing. IEEE Transactions on Quantum Engineering **4**, 1–32 (2023). https://doi.org/10.1109/TQE.2023.3253761
17. Manzano, A., Musso, D., Leitao, A.: Real Quantum Amplitude Estimation. EPJ Quantum (2 2023). https://doi.org/10.1140/epjqt/s40507-023-00159-0
18. Michielsen, K., Nocon, M., Willsch, D., Jin, F., Lippert, T., De Raedt, H.: Benchmarking gate-based quantum computers. Computer Physics Communications **220**, 44–55 (2017). https://doi.org/https://doi.org/10.1016/j.cpc.2017.06.011, https://www.sciencedirect.com/science/article/pii/S0010465517301935
19. Mills, D., Sivarajah, S., Scholten, T.L., Duncan, R.: Application-Motivated, Holistic Benchmarking of a Full Quantum Computing Stack. Quantum **5**, 415 (Mar 2021). https://doi.org/10.22331/q-2021-03-22-415, https://doi.org/10.22331/q-2021-03-22-415
20. Pelofske, E., Bärtschi, A., Eidenbenz, S.: Quantum Volume in Practice: What Users Can Expect From NISQ Devices. IEEE Transactions on Quantum Engineering **3**, 1–19 (2022). https://doi.org/10.1109/TQE.2022.3184764
21. Plekhanov, K., Rosenkranz, M., Fiorentini, M., Lubasch, M.: Variational quantum amplitude estimation. Quantum **6**, 670 (mar 2022). https://doi.org/10.22331/q-2022-03-17-670, https://doi.org/10.22331/q-2022-03-17-670
22. Preskill, J.: Quantum computing in the nisq era and beyond. Quantum **2** (8 2018). https://doi.org/10.22331/q-2018-08-06-79
23. Proctor, T.J., Rudinger, K.M., Young, K.C., Nielsen, E., Blume-Kohout, R.: Measuring the capabilities of quantum computers. Nature Physics **18**, 75 – 79 (2020). https://doi.org/https://doi.org/10.1038/s41567-021-01409-7
24. Robert, C.P., Casella, G.: Monte Carlo Integration, pp. 71–138. Springer New York, New York, NY (1999). https://doi.org/10.1007/978-1-4757-3071-5_3
25. Suzuki, Y., Uno, S., Raymond, R., Tanaka, T., Onodera, T., Yamamoto, N.: Amplitude estimation without phase estimation. Quantum Information Processing **19** (01 2020). https://doi.org/10.1007/s11128-019-2565-2
26. Tanaka, T., Suzuki, Y., Uno, S., Raymond, R., Onodera, T., Yamamoto, N.: Amplitude estimation via maximum likelihood on noisy quantum computer. Quantum Information Processing **20** (9 2021). https://doi.org/10.1007/s11128-021-03215-9
27. Tanaka, T., Uno, S., Onodera, T., Yamamoto, N., Suzuki, Y.: Noisy quantum amplitude estimation without noise estimation. Phys. Rev. A **105**, 012411 (Jan 2022). https://doi.org/10.1103/PhysRevA.105.012411
28. Uno, S., Suzuki, Y., Hisanaga, K., Raymond, R., Tanaka, T., Onodera, T., Yamamoto, N.: Modified grover operator for quantum amplitude estimation. New Journal of Physics **23**(8) (aug 2021). https://doi.org/10.1088/1367-2630/ac19da, https://dx.doi.org/10.1088/1367-2630/ac19da
29. Wack, A., Paik, H., Javadi-Abhari, A., Jurcevic, P., Faro, I., Gambetta, J., Johnson, B.: Quality, Speed, and Scale: three key attributes to measure the performance of near-term quantum computers (10 2021), arXiv preprint arXiv:2110.14108
30. Wack, A., McKay, D.: (Nov 2023), https://research.ibm.com/blog/quantum-metric-layer-fidelity

ICCS Camera Ready Version 2024
To cite this paper please use the final published version:
DOI: 10.1007/978-3-031-63778-0_16